USE OF LEAD ISOTOPES IN DEVELOPING CHRONOLOGIES FOR RECENT SALT-MARSH SEDIMENTS

Andrew C. Kemp[1, 2*], Christopher K. Sommerfield[3], Christopher H. Vane[4], Benjamin P. Horton[5], Simon Chenery[4], Shimon Anisfeld[1] and Daria Nikitina[6]

[1] *School of Forestry and Environmental Studies, Yale University, New Haven, CT 06511, USA*

[2] *Yale Climate and Energy Institute, New Haven, CT 06511, USA*

[3] *College of Earth, Ocean, and Environment, University of Delaware, Lewes, DE 19958, USA*

[4] *British Geological Survey, Kingsley Dunham Center, Keyworth, Nottingham NG12 5GG, UK*

[5] *Sea Level Research, Department of Earth and Environmental Science, University of Pennsylvania, Philadelphia, PA 19104, USA*

[6] *Department of Geology and Astronomy, West Chester University, West Chester, PA 19380, USA*

** Corresponding author. andrew.kemp@yale.edu tel: 203 436 3978*

ABSTRACT

Dating of recent salt-marsh sediments is hindered by the radiocarbon plateau and the moving ~100 year window of ^{210}Pb accumulation histories. Introduction of anthropogenic Pb to the environment is a means to date salt-marsh sediment deposited over the last 200 years by correlating downcore changes in concentration and isotopic ratios to historical production and consumption. We investigated use of Pb as a chronometer in a core of salt-marsh sediment from New Jersey, USA. Changes in Pb concentration identified horizons at AD 1875, 1925, 1935 and 1974 that correspond to features of historic U.S Pb production and consumption. Stable lead isotopes (^{206}Pb:^{207}Pb) constrained ages at AD 1827, 1857 and 1880, reflecting Pb production in the Upper Mississippi Valley with its unusual isotopic signature and at AD 1965 and 1980 from leaded gasoline. These chronostratigraphic markers of fixed dates provide precise constraints on sediment age during part of the radiocarbon plateau. Use of Pb to develop chronologies for recent salt-marsh sediment enables high resolution records of sea-level change to extend beyond the period of instrumental records and to better constrain the initiation of accelerated sea-level rise.

1 INTRODUCTION

Modern rates of sea-level rise recorded by tide gauges (Douglas, 2001; Woodworth et al., 2009; Church and White, 2011) and, more recently, satellites (Cabanes et al., 2001; Leuliette and Miller, 2009) exceed those of the last 2000 to 4000 years estimated using geological techniques (Donnelly et al., 2004; Gehrels et al., 2005; Engelhart et al., 2009). The limited duration and distribution of instrumental records hinders attempts to constrain the timing and magnitude of this apparent acceleration. High-resolution (decadal and decimeter scale) reconstructions of relative sea level (RSL) using salt-marsh sediments bridge the gap between instrumental and geological records and suggest that the increased rate of sea-level rise was initiated in the late 19th century or early 20th century (Donnelly et al., 2004; Gehrels et al., 2005; Gehrels et al., 2008; Kemp et al., 2009; Kemp et al., 2011).

Salt-marsh sediments provide detailed archives of RSL change because their spatial distribution is intimately linked to the tidal frame (Chapman, 1960). Salt marshes track moderate rates of RSL rise by accreting vertically through a combination of vegetative growth and detrital sedimentation of organic and inorganic (mineral) particles (Orson et al., 1998). The resulting sedimentary sequences can form continuous accumulations of salt-marsh peat that are well suited to producing high-resolution RSL reconstructions if accurate and precise chronologies are developed.

Abundant organic material (including plant macrofossils) in salt-marsh sediments has made radiocarbon (^{14}C) dating the principal means of determining the age of sea-level

58 indicators (Tornqvist et al., 1992; van de Plassche et al., 1998; Shennan and Horton,
59 2002; Tornqvist et al., 2004; Engelhart et al., 2011). Difficulties with this technique
60 hinder its application to sediments younger than about 350 years. Between AD 1650 and
61 1950, a plateau in the ^{14}C calibration curve caused by natural variability in atmospheric
62 ^{14}C production hampers chronological interpretation by producing multiple calendar ages
63 for a single sample (Reimer and Reimer, 2007). Since AD 1950 introduction of
64 anthropogenic ^{14}C from above-ground testing of nuclear weapons has significantly
65 altered atmospheric ^{14}C concentration (Shotyk et al., 2003; Hua and Barbetti, 2004;
66 McGee et al., 2004). Although new approaches to ^{14}C dating have increased its
67 usefulness for estimating the age of recent sediments (Marshall et al., 2007; Hua, 2009),
68 studies seeking to provide detailed records of recent RSL changes from salt-marshes rely
69 upon alternative techniques to achieve the desired temporal resolution for the last 350
70 years.
71
72 The most widely used radionuclide for estimating the accumulation rate and relative age
73 of recent salt-marsh sediments is ^{210}Pb (Gehrels et al., 2005; Kemp et al., 2009). Use of
74 ^{210}Pb as a sediment chronometer involves assumptions regarding how ^{210}Pb is delivered
75 from the atmosphere to sediments (Robbins, 1978; Appleby and Oldfield, 1992; Appleby,
76 2001). The relative amount of atmospheric rainout versus tide-water sources of ^{210}Pb to
77 salt marshes cannot be determined with certainty, therefore ^{210}Pb-based sediments age
78 estimates are corroborated by independent means. Radiocesium (^{137}Cs) is most
79 frequently used in this capacity as it provides an absolute time marker for peak fallout in
80 AD 1963-64 (Ritchie and McHenry, 2000). A limitation of ^{210}Pb geochronology is that it

81 is restricted to the last 100 to 120 years, and this range moves forward each year leaving a
82 growing "*chronological vacuum*" (Gale, 2009).
83
84 Stable Pb isotopes can extend sediment chronologies developed using ^{210}Pb and ^{137}Cs,
85 and narrow the crucial gap (approximately AD 1650 to 1900) between time scales
86 covered by these radionuclides and ^{14}C geochronology. The age and geological history
87 of mineral deposits results in Pb ores having differing isotopic compositions (Russell and
88 Farquhar, 1960; Chow and Earl, 1972). During industrial processes (including
89 production and consumption of leaded gasoline), there is minimal fractionation of Pb
90 isotopes and emissions preserve the Pb isotopic signature of the ore from which they
91 were derived (Ault et al., 1970; Doe, 1970). Prior to AD 1979 as much as 19.6 x 10^9 kg
92 of Pb was added to the atmosphere from global anthropogenic emissions (Nriagu, 1979),
93 primarily high-temperature industrial activities and combustion of leaded gasoline (Kelly
94 et al., 2009). The atmospheric residence time of Pb aerosols permits their dispersal and
95 subsequent deposition over continental-scale distances by prevailing winds (Sturges and
96 Barrie, 1987; Wu and Boyle, 1997; Bollhöfer and Rosman, 2000, 2001), as shown by
97 measurements at sites distal to source regions, such as Greenland (Rosman et al., 1993;
98 Hong et al., 1994), Bermuda (Shen and Boyle, 1987; Kelly et al., 2009), and deep ocean
99 basins (Schaule and Patterson, 1981; Shen and Boyle, 1987; Hamelin et al., 1997; Wu et
100 al., 2010). There is close agreement between the timing of emissions and deposition
101 (Graney et al., 1995). As the precision of analytical measurements is smaller than the
102 variability of source material (Shen and Boyle, 1987; Chillrud et al., 2003), ratios of
103 stable Pb isotopes preserved in sedimentary archives can distinguish among different

104 sources of anthropogenic Pb (Shotyk et al., 1998; Kamenov et al., 2009). Most
105 investigations of historical Pb deposition used independent chronological control or
106 correlation with dated sedimentary records (Lima et al., 2005b) to describe the timing of
107 Pb contamination and to apportion sources of pollution (Edgington and Robbins, 1976;
108 Graney et al., 1995; Cochran et al., 1998; Marcantonio et al., 2002; Lima et al., 2005b;
109 Kamenov et al., 2009). Alternatively, changing concentrations and ratios of Pb isotopes
110 measured in sediments can be ascribed to historical variations in Pb production and
111 consumption with well-established ages (Shen and Boyle, 1987; Graney et al., 1995;
112 Farmer et al., 2001; Marcantonio et al., 2002; Chillrud et al., 2004; Lima et al., 2005b;
113 Gehrels et al., 2008; Kelly et al., 2009; Vane et al., 2011). Anthropogenic Pb emissions
114 are thus a potentially valuable source of chronological control on salt-marsh accretion
115 history over the last 200 years in the northeastern U.S.
116
117 In this paper we investigate Pb concentrations and isotopes (^{210}Pb with ^{137}Cs and
118 ^{206}Pb:^{207}Pb) as a chronometer of recent salt-marsh sediments using a sediment core from
119 a U.S. Mid-Atlantic salt marsh. We discuss the application of anthropogenic Pb
120 chronostratigraphic markers for future studies seeking to develop high-resolution RSL
121 reconstructions from salt marshes in this region.
122
123 **2 REGIONAL SETTING**
124 Sediment core BB1was obtained from a salt marsh in northern Barnegat Bay (New
125 Jersey), an archetype back-barrier coastal lagoon in the U.S. Mid-Atlantic region (Figure
126 1). The 280 km^2 bay, which is fringed by *Spartina alterniflora* salt marsh, has a mean

depth of 1.5 m and a mean tidal range that decreases from 1.4 m at the inlet to 0.3 m at its northern and southern limits. Although the bay and its extensive marshes have a history of human impacts, including grid ditching (Kennish, 2001) and eutrophication (Kennish et al., 2007), much of the marsh accretes vertically unobstructed by human influences. Barnegat Bay lacks a large source of river sediment, therefore supply of allochthonous mineral sediment to the marsh platform is low compared to Mid-Atlantic river-estuarine marshes. Consequently, salt-marsh accretion rates determined by ^{210}Pb and ^{137}Cs measurements at sites throughout the bay are low (0.2–0.3 cm/yr) compared to minerogenic marshes in the region (Velinsky et al., 2011). Importantly, supply of ^{210}Pb to Barnegat Bay salt marshes is derived mostly (if not exclusively) from direct atmospheric deposition, an ideal condition for developing chronologies of anthropogenic Pb isotopes. Core BB1 was selected because it exhibited concordant ^{210}Pb and ^{137}Cs chronologies, and was sufficiently long (94 cm) to capture the full post-industrial record of anthropogenic Pb fallout.

3 METHODS

Sediment cores from Barnegat Bay salt marshes were collected in 2009 as part of an unrelated study of historical sediment and nutrient loading (Velinsky et al., 2011). Using a push-piston core (10 cm diameter) system designed to minimize compaction, BB1 was collected in a high-marsh floral zone (short-form *Spartina alterniflora*), 25 m landward of Reedy Creek, at a surveyed elevation of 0.10 m NAVD 88 (Figure 1). Duplicate cores of BB1 were recovered, one for radionuclide and chemical analysis and another for

149 stratigraphic description and archiving. Cores were capped in the field and transported to
150 the laboratory for processing.
151
152 *3.1 Sample preparation*
153 The core for radionuclide and chemical analysis was sectioned in 2 cm thick intervals.
154 Samples were weighed wet, dried at 110°C for 24 hours in a convection oven, and
155 weighed again dry to determine gravimetric water content, porosity, and dry-bulk density
156 (Bennett and Lambert, 1971). Approximately 20–60 g of dried sediment was ground to a
157 homogeneous powder, and a 4 g aliquot was combusted in a muffle furnace to determine
158 loss on ignition (LOI) following methods described in (Heiri et al., 2001). LOI quantified
159 the relative proportion of organic (combustible) and mineral (residual ash) materials in
160 the sediments. Gravimetric and LOI data were used to interpret the downcore
161 radionuclide and stable Pb profiles. Each sample between depths of 0 and 94 cm (n=47)
162 was analyzed for Pb concentrations and stable Pb isotopes, whilst only samples from 0 to
163 36 cm (n=18) were analyzed for ^{210}Pb and ^{137}Cs activity.
164
165 *3.2 Radionuclide Measurement*
166 Powder samples were sealed in a 60 ml plastic jar, stored for at least 30 days to ensure
167 equilibrium between ^{226}Ra and ^{214}Bi, and then counted for 24 hours on Canberra Model
168 2020 low-energy Germanium detectors. Measurements of ^{210}Pb ($t_{1/2}$=22.3 years) and
169 ^{137}Cs ($t_{1/2}$=30.1 years) activity were made by gamma spectroscopy of the 46.5 and 661.6
170 keV photopeaks, respectively (reviewed by (Cutshall et al., 1983; Wallbrink et al., 2002).
171 The full-energy peak efficiency of these detectors is 4% at 46.5 keV and 1% at 661.6

keV, and the minimum detectable activity for photopeaks of ^{210}Pb and ^{137}Cs is approximately 2–3 Bq/kg. Excess ^{210}Pb activity was determined by subtracting the activity of its parent nuclide (^{214}Bi at 609.3 keV) from the total activity ($^{210}Pb_{xs}=^{210}Pb_{tot} - ^{214}$Bi). Detector efficiencies were determined using the NIST Ocean Sediment Standard Reference Material 4357 (Inn et al., 2001). The standard (a sediment powder) and core material were counted in an identical geometry, thus negating a self-absorption correction for ^{210}Pb. Confidence limits for radionuclide data are computed as the propagated one-sigma background, calibration, and counting errors.

3.3 Radionuclide chronology

Two models were used to develop ^{210}Pb chronologies for core BB1. Detailed descriptions of both approaches are available in the literature (Robbins, 1978; Appleby and Oldfield, 1992; Appleby, 2001). The Constant Initial Concentration (CIC) model assumes that the *specific activity* (dpm/g) of excess ^{210}Pb deposited on a marsh surface remained constant through time and that variations in the rate of sediment deposition do not influence the initial activity of excess ^{210}Pb. The Constant Rate of Supply (CRS) ^{210}Pb model relates sediment age and depth by assuming that the *depositional flux* of ^{210}Pb (Bq/cm^2/yr) to a marsh surface was constant. Peak ^{137}Cs at AD 1963-64 provided an independent means to corroborate ^{210}Pb accumulation histories.

3.4 Determination of Pb and Sb concentrations and ratios of stable Pb isotopes

In preparation for determining concentrations of stable Pb isotopes and Sb, 0.25 g of powdered sediment was dissolved by a HF/$HClO_4$/HNO_3 mixed concentrated acid attack

195 in Savillex™ PFA vials. Samples were reconstituted in dilute nitric acid and diluted to:
196 (i) within the calibration range of Pb and Sb chemical standards for concentration
197 measurements; and (ii) within the pulse counting range (< 1Mcps) of the ICP-MS for
198 isotope ratio measurements.
199
200 Concentration and isotope ratio determinations were made using a quadrupole ICP-MS
201 instrument (Agilent 7500c) with a conventional glass concentric nebuliser. The long term
202 2σ precision for the BCR-2 reference material used for quality control, which has a total
203 Pb concentration of 11 mg/kg was $^{207/206}Pb = 0.0008$, $^{208/206}Pb = 0.0020$, based on n=32
204 replicates over 29 months and a mean accuracy, relative to the published values of (Baker
205 et al., 2004), within that error. Data (raw isotope intensity count rates) were processed
206 off-line using Microsoft Excel spreadsheets. Processing consisted of: (i) removal of
207 background; (ii) calculation of isotope ratios; (iii) determination of mass bias correction
208 factor from defined isotope ratios of SRM981; (iv) application of mass bias factors
209 derived from SRM981 using external standard-sample-standard bracketing; and (v)
210 optional further correction for linearity of ratio with signal strength.
211
212 *3.5 Identifying Pb chronostratigraphic markers*
213 We identified nine historical features of U.S. Pb production and consumption that could
214 be used as chronostratigraphic markers to estimate sediment age in core BB1 (Table 1;
215 Figure 2). Four were recognized in Pb concentration and five in ^{206}Pb:^{207}Pb ratios.
216 Changes in production and consumption are assumed to have caused a corresponding
217 change in Pb emissions that were transported through the atmosphere and deposited on

Comment [ak1]: What are the units for these numbers? I am assuming mg/kg

218 the salt-marsh surface within a few years (Graney et al., 1995) and without isotopic
219 fractionation (Ault et al., 1970). As emissions per unit of production or consumption are
220 likely to have changed over time, trends rather than absolute values are the basis for
221 recognizing these features in core BB1. The stratigraphic context of core BB1, and the
222 ordering of samples, provides an appropriate sedimentary constraint for interpreting
223 downcore changes in Pb concentration and ^{206}Pb:^{207}Pb as being reliably correlated to the
224 nine historical features. We used downcore concentration of Sb to distinguish between
225 changes before and after the widespread introduction of automobiles around AD 1920
226 because it has low abundance in pristine environments, similar environmental behavior to
227 Pb (Shotyk et al., 2005) and is a high-contrast marker for aerial deposition from road
228 traffic (Gomez et al., 2005; Amarasiriwardena and Wu, 2011; Fujiwara et al., 2011). Its
229 association with automotive emissions makes it useful for confirming interpretations of
230 Pb data as being related (or unrelated) to leaded gasoline.
231
232 **4 RESULTS**
233 *4.1 ^{210}Pb and ^{137}Cs activities and chronology*
234 Radionuclides were measured in the upper 36 cm of core BB1 (Figure 3a). Excess ^{210}Pb
235 increased near-exponentially upcore from 1.3 Bq/kg at 31 cm to 166 Bq/kg at the top, a
236 pattern consistent with steady-state sediment accumulation and radioactive decay. The
237 accretion rate based on regression of the decay profile is 0.25 cm/yr. The ^{137}Cs profile
238 (Figure 3b) broadly mirrors the record of ^{137}Cs atmospheric fallout in northern temperate
239 latitudes (Warneke et al., 2002). Activity of ^{137}Cs increased upcore from the depth of
240 first occurrence above the detection limit (20–22 cm) to a peak centered at 9 cm, above

241 which activity decreased to the core top. The accretion rate based on the AD 1963-64
242 peak is 0.25 cm/yr, identical to the ^{210}Pb-based rate. Accumulation histories were
243 developed for BB1 using the CIC and CRS models (Figure 3). This yielded age dates
244 from AD 1901 to the time of core collection (AD 2009).
245
246 *4.2 Total Pb and Sb concentration and ratios of stable Pb isotopes*
247 The average Pb concentration of samples between 93 cm and 43 cm in BB1 was 11.2
248 mg/kg and represents background levels (Figure 2c). Samples at 41, 39 and 37 cm had an
249 average Pb concentration of 23.8 mg/kg. From 35 cm to 21 cm, it increased from 20.5 to
250 93.3 mg/kg. The interval from 21 cm to 17 cm was characterized by a decline in Pb
251 concentration to 76.5 mg/kg. Maximum Pb concentration (164 mg/kg) occurred at 9 cm
252 and declined to 65.8 mg/kg at the modern marsh surface. Antimony (Sb) concentrations
253 paralleled those of Pb (Figure 2c). Below 41 cm, total Sb concentration was 0.09-0.36
254 mg/kg. It increased to a peak of 1.44 mg/kg at 23 cm before declining to 1.13 mg/kg at
255 13 cm. Maximum Sb concentration was at 9 cm (1.63 mg/kg) and declined to 0.86 mg/kg
256 at the core top.
257
258 Measured concentrations of Pb isotopes are expressed as ratios. From 93 cm to 51 cm
259 ^{206}Pb:^{207}Pb varied between 1.197 and 1.226 (Figure 2d). It reached a minimum of 1.174
260 at 43 cm before increasing to a maximum value of ~1.234 at 33-35 cm. There was a
261 decline in ^{206}Pb:^{207}Pb between 33 cm and 11 cm (1.186) prior to another increase to 1.207
262 at 9 cm and a subsequent decrease to the modern marsh surface value of 1.200.
263

5 DISCUSSION

5.1 ^{210}Pb and ^{137}Cs accumulation histories

The CRS model, which was originally developed for lake sediments (Krishnaswamy et al., 1971) and only later applied to salt marshes (McCaffery and Thomson, 1980), is best suited to marshes that sequester ^{210}Pb primarily by direct atmospheric deposition. In highly allochthonous marsh systems, particle-borne ^{210}Pb transported tidally to the marsh platform supplies activity in addition to that derived atmospherically. Because flux of tidal ^{210}Pb to the sediment surface is highly discontinuous, the steady-state assumption of the CRS model is frequently contradicted in minerogenic marshes. In Barnegat Bay marshes, the sediment inventory of excess ^{210}Pb is comparable to the theoretical inventory supported by the regional atmospheric flux, suggesting that tidal supply of ^{210}Pb is minimal (Velinsky et al., 2011).

Comment [ak2]: But its actually CIC that agrees with the 137Cs depth.

Age-depth relationships predicted by the CIC and CRS ^{210}Pb models were in agreement (Figure 3c), suggesting that the accretion rate at site BB1 has been roughly constant over the past century. The CRS model is particularly sensitive to sediment compositional changes that influence the cumulative inventory of excess ^{210}Pb, and this explains minor divergences between the CRS and CIC models where the core changes from rooted to non-rooted muddy peat. Considering the different assumptions associated with ^{210}Pb modeling and ^{137}Cs chronology, the concordance of the methods for core BB1 indicates that the sediment column is unmixed and stratigraphically complete.

5.2 Pb concentrations

Four features of historic U.S. Pb production and consumption (Figure 4a) are recognized in BB1 (Figure 2c; Table 1). Prior to AD 1935, U.S. consumption of Pb was equal to primary production. Pb production and consumption increased dramatically in the second half of the 19th century, although some anthropogenic Pb was released to the atmosphere much earlier in North America (Heyl et al., 1959) and Europe (Rosman et al., 1997). During this period inefficient furnaces and smelting coupled with development of taller stacks caused large amounts of Pb to be released to the atmosphere (Nriagu, 1998). National Pb production increased from an annual average of 15,703 tons between AD 1830 and AD 1871 to 106,218 tons in AD 1881 (Figure 4a). The pronounced increase in Pb concentration at 33 ± 3 cm in BB1 represents this onset of large-scale, national Pb production and consumption. To accommodate uncertainty in establishing the timing of this change we assigned the sample a date of AD 1875 ± 5 years. The vertical uncertainty reflects difficulty in attributing the start of a trend to a specific sample (those at 35, 33 or 31 cm could represent this event). U.S. Pb production peaked in AD 1925 (620,913 tons) and consumption peaked in AD 1928 which is recorded at 21 cm in BB1 with an estimated uncertainty of ± 5 years.

The period from AD 1933 to AD 1962 was characterized by lower Pb production (average 319,244 tons annually). Coincident with the Great Depression, Pb consumption declined from 683,655 tons in AD 1930 to 378,024 in AD 1932 (Figure 4a). However, it had recovered to 952,544 tons in AD 1941. This divergence between production and consumption was a consequence of increasing consumption of secondary and imported Pb. A minimum Pb concentration at 17 cm in BB1 was interpreted as corresponding to

310 the consumption decline and assigned a date of AD 1935 ± 6 years. A second peak in Pb
311 production (602,253 tons) and consumption (1,450,976 tons) occurred in AD 1974, since
312 when it followed a declining trend. Peak Pb concentration in BB1 at 9 cm was assigned a
313 date of AD 1974 ± 5 years.
314
315 *5.2 Pre-AD 1920 stable Pb isotopes*
316 Prior to the 1920s, the principal source of anthropogenic Pb released to the atmosphere
317 was industrial activity. Between AD 1830 and AD 1870 most U.S. Pb (average 79% ±
318 17%, 1σ) was sourced from the Upper Mississippi Valley (UMV) Pb and Zn district
319 (Figure 4b), principally in Illinois, Iowa and Wisconsin where it was smelted close to
320 mines (Heyl et al., 1959). Three features of historic UMV Pb production are recognized
321 in BB1 (Figure 2c; Table 1). UMV ores are distinctive because of their unusual isotopic
322 composition with high (1.3 to 1.5) ^{206}Pb:^{207}Pb values (Heyl et al., 1966; Doe and
323 Delevaux, 1972; Heyl et al., 1974). Changes in ^{206}Pb:^{207}Pb measured in BB1 likely
324 record changes in UMV Pb production because of the location of Barnegat Bay relative
325 to this source and prevailing winds which carried UMV lead to regions north and south of
326 New Jersey (Marcantonio et al., 2002; Lima et al., 2005b) as well as to Bermuda (Kelly
327 et al., 2009). Therefore ^{206}Pb:^{207}Pb measurements in New Jersey salt-marsh sediments
328 can potentially be used as chronostratigraphic markers. Dates ascribed to depths in core
329 BB1 using Pb concentrations are stratigraphic constraints on the timing of ^{206}Pb:^{207}Pb
330 changes (Figure 2). Samples below 43 cm show variability but do not represent
331 anthropogenic Pb inputs because these samples have background Pb concentrations. Sb
332 concentrations confirm that changes associated with UMV Pb production took place

333 before the widespread use of automobiles because vehicles are a major source of
334 anthropogenic Sb.
335
336 UMV Pb production increased rapidly between AD 1824 (301 metric tons) and AD 1830
337 (5,416 metric tons) (Heyl et al., 1959). We assigned the initial increase in measured
338 ^{206}Pb:^{207}Pb at 41 cm a date of AD 1827 ± 5 years to correspond with the start of UMV Pb
339 production. Peak production (approximately 25,000 metric tons annually) occurred from
340 AD 1845 to AD 1847 (Heyl et al., 1959). Peak ^{206}Pb:^{207}Pb in BB1 was at 34 cm (± 2
341 cm). Measured ^{206}Pb:^{207}Pb peaks in sediment may better reflect maximum proportional
342 contribution than maximum absolute production (in tons) because this is the time when
343 dilution of the UMV signal from other sources is minimal. UMV Pb made its maximum
344 relative contribution to national production in AD 1857 and AD 1858. Therefore the
345 peak at 34 cm was assigned a date of AD 1857.
346
347 Production of Pb in the UMV declined during the late 19th century from 47% of national
348 output in AD 1871 to less than 5% by AD 1878. It had fallen to AD 1827 levels by the
349 middle of the AD 1880s and by AD 1895 to 1905 average annual production was 180
350 tons annually equating to <1% of national production. We assigned a date of AD 1880 ±
351 20 years to this decline. Identifying its effect on measured ^{206}Pb:^{207}Pb in BB1 is
352 challenging; a minimum occurred at 21 cm although the decline to background values
353 (approximately 1.207) occurred at 26 cm. This is further complicated by rapidly
354 increasing national production which masks and overprints changes in the UMV. We
355 assigned the sample at 23 cm a date of AD 1880 ± 20 years with an added vertical range

356 of ± 3 cm to capture the uncertainty described. Disassociation of these changes with Sb
357 concentrations suggests that they were not caused by emissions from automotive
358 transport and occurred prior to AD 1920. Although absolute production of UMV Pb
359 increased during the 20th century (e.g. World War One) it did not exceed 1.5% of the
360 national total.
361
362 Following isotopic analysis of other potential sources including coal and Pb from other
363 regions, they concluded that this change corresponded to historical Pb production in the
364 UMV. Marcantonio et al. (2002) showed that Chesapeake Bay estuarine sediments
365 deposited in the middle of the 19th century had a broad, shallow ^{206}Pb:^{207}Pb peak (Figure
366 5a). Great Lake sediments dated using ^{210}Pb and pollen had peak anthropogenic
367 ^{206}Pb:^{207}Pb in AD 1883 in Erie, AD 1863 in Michigan and AD 1895 in Ontario (Graney
368 et al., 1995). In Florida, a core of peat dated using ^{210}Pb and ^{14}C did not show significant
369 increase in ^{206}Pb:^{207}Pb during the 19th century (Kamenov et al., 2009). Annually-banded
370 corals provide an independently dated archive of historical Pb deposition (Shen and
371 Boyle, 1987). At John Smith's Bay (Bermuda), ^{206}Pb:^{207}Pb increased from 1.187 in AD
372 1826 to 1.211 in AD 1854, which was attributed to UMV Pb production (Kelly et al.,
373 2009). In Rhode Island, (Lima et al., 2005b; Lima et al., 2005a) identified an increase in
374 measured ^{206}Pb:^{207}Pb from 1.211 (AD 1815) to 1.325 (AD 1842) in lake sediments dated
375 using varve counting confirmed by ^{210}Pb with ^{137}Cs peaks (Figure 5a). They concluded
376 that differences among timing of mid 19th century ^{206}Pb:^{207}Pb maximums are caused by
377 problems with age models and that the peaks actually represent simultaneous deposition
378 of UMV Pb. Differences in the magnitude of ^{206}Pb:^{207}Pb peaks were proposed to reflect

379 mixing of multiple, spatially variable Pb sources (Lima et al., 2005b). For example,
380 prevailing winds caused less UMV Pb to be deposited in the Chesapeake Bay than in
381 New England and to have been absent in Florida. Consequently, Lima et al. (2005a)
382 proposed that three chronological horizons (initiation, peak and decline) associated with
383 deposition of UMV Pb could be identified in sedimentary archives in the northeastern
384 U.S. (Figure 5). These horizons narrow the chronological hiatus between radiocarbon
385 and ^{210}Pb accumulation histories.
386
387 *5.3 Post-AD 1920 stable Pb isotopes*
388 Two ^{206}Pb:^{207}Pb features associated with leaded gasoline are recognized in BB1. Leaded
389 gasoline was a significant source of anthropogenic Pb following its introduction in AD
390 1923 (Facchetti, 1989; Nriagu, 1990). Peak U.S. production occurred in AD 1970
391 (exceeding 250,000 tons annually; Figure 4c). Following the Clean Air Act (AD 1970)
392 consumption of leaded gasoline declined to 17,000 tons in AD 1988 (Nriagu, 1990). By
393 AD 1993 U.S. Pb emissions from gasoline were 1% of those in AD 1970 (Bollhöfer and
394 Rosman, 2001). Up to two thirds of Pb added to gasoline entered the atmosphere as fine
395 particulate matter that was transported long distances through the atmosphere (Facchetti,
396 1989). The Pb ore(s) used in gasoline production and released to the atmosphere varied
397 over time and also among regions in the U.S. depending on the mixture used by each
398 manufacturer (Shirahata et al., 1980; Facchetti, 1989; Rosman et al., 1993; Graney et al.,
399 1995), although geological records of Pb deposition and direct measurements of
400 atmospheric Pb isotopes suggest that a regional-scale patterns can be discerned for the
401 northeastern U.S. (Marcantonio et al., 2002).

From the introduction of leaded gasoline until the mid-1960s, ^{206}Pb:^{207}Pb values declined slightly as non-radiogenic Pb was added to gasoline (Lima et al., 2005b). Direct measurements of the isotopic composition of gasoline or atmospheric emissions are sparse for this period. The ALAS model (Hurst, 2000) suggests that ^{206}Pb:^{207}Pb in gasoline declined from 1.175 in the 1920s to 1.145 in the mid-1960s (Figure 5c). These values are in agreement with atmospheric measurements for eastern North America and California of 1.15 in AD 1967 (Shirahata et al., 1980; Rosman et al., 1993). In Rhode Island lake sediments, Lima at al. (2005a) reported a decline from 1.197 in AD 1922 to 1.190 in AD 1964 (Figure 5b). Similarly, sediments from the Chesapeake Bay (core MD) showed a ^{206}Pb:^{207}Pb decline from 1.207 in AD 1898 to a minimum of 1.193 in AD 1956. Coral records from Bermuda showed no trend in isotopic ratio (Kelly et al., 2009). Decreased ^{206}Pb:^{207}Pb from 19 cm to 11 cm in BB1 (Figure 2d) was caused by the introduction (and dominance until the mid 1960s) of leaded gasoline with a relative constantly isotopic signature of 1.165 (Hurst, 2000; Lima et al., 2005b). This had the effect of diluting other contributions resulting in the minima of 1.185 at 11cm in BB1. We assigned this ^{206}Pb:^{207}Pb minimum a date of AD 1965 ± 5 years (Table 1; Figure 2d and 6a).

After approximately AD 1965, ^{206}Pb:^{207}Pb ratios in gasoline increased (Figure 5) because Pb ores from Missouri were increasingly used (Graney et al., 1995; Hurst, 2000). Shirahata et al. (1980) showed an increase in measured atmospheric ^{206}Pb:^{207}Pb from 1.15 in AD 1967 to 1.23 in AD 1977, whilst the averaged record of Rosman et al. (1993)

showed a U.S. aerosol peak of 1.22 in AD 1980. Peak ^{206}Pb:^{207}Pb in Greenland snow occurred between AD 1972 and AD 1984 (Rosman et al., 1993). Since the decline of leaded gasoline, no clear regional pattern of changing ^{206}Pb:^{207}Pb values has emerged and records show variability since AD 1980 (Figure 5). The ^{206}Pb:^{207}Pb peak in BB1 at 7 cm was given a date of AD 1980 ± 5 years (Table 1; Figure 6). The sedimentary record from Rhode Island showed a ^{206}Pb:^{207}Pb rise from 1.192 in AD 1966 to a peak of 1.205 in AD 1981 (Lima et al., 2005b). In the Chesapeake Bay, ^{206}Pb:^{207}Pb values increased from 1.197 in AD 1967 to a peak of 1.204 in AD 1981. Bermudan corals show a pronounced increase in ^{206}Pb:^{207}Pb between AD 1964 (1.174 and 1.183 at John Smith's Bay and North Rock respectively) and AD 1977 (1.191 and 1.205).

5.4 Development of age-depth profiles for BB1

We used the nine samples with ages estimated from Pb concentrations or ^{206}Pb:^{207}Pb (Table 1) as the input for an age-depth model (Figure 6). In addition, year of core collection (AD 2009) was added as a surface data point (0-1 cm depth), but was not specified as a fixed constraint. The sample at 34 cm was assigned a date of AD 1857 ± 5 years in favor of when the UMV made its maximum proportional contribution to national Pb production. Results from ^{210}Pb and ^{137}Cs were not included. Age-depth models use dated samples to provide downcore age estimates with sample-specific uncertainty at 1 cm intervals. We applied the "Clam" model of (Blaauw, 2010) executed in R and using a locally weighted spline. Model age uncertainties (2σ) ranged from 4 to 15 years with an average of 8 years. The Clam model estimates an approximately linear rate of sediment accumulation in core BB-1 since AD 1827 (lowest date), although a period of slightly

448 reduced sedimentation is predicted between approximately AD 1910 and AD 1940
449 (Figure 6b). The age-depth model developed using CIC ^{210}Pb accumulation lies within
450 the 95% confidence interval of the Clam model at all depths. This agreement suggests
451 that ^{210}Pb accumulation histories developed from high salt-marsh peat are accurate.
452
453 *5.5 Implications for dating the onset of accelerated sea-level rise in salt marsh sediments*
454 Accelerated sea-level rise recorded by tide gauges is often reported as occurring at
455 approximately AD 1920 (Church and White, 2006). Reconstructions of RSL from salt-
456 marsh sediment can extend instrumental histories and resolve the timing of this important
457 change if adequate chronologies can be developed. The nine, regional,
458 chronostratigraphic markers recognized in salt-marsh sediment from New Jersey using Pb
459 concentrations and stable Pb isotopic ratios help meet the need for a dating technique in
460 the hiatus between ^{14}C and ^{210}Pb. These markers dating back to AD 1827 are of fixed age
461 and unaffected by the moving, 100 year window limitation of ^{210}Pb. In the near future
462 tide-gauge records will span a longer interval than can be resolved using ^{210}Pb. Indeed,
463 some tide-gauge records in the northeastern U.S. already exceed 100 years (e.g. New
464 York City, Philadelphia and Baltimore). Therefore concentrations and isotopic ratios of
465 Pb are useful to use salt-marsh sediment to bridge the gap between instrumental and
466 geological records of RSL change.
467
468 **6 Conclusions**
469 Reconstructions of sea-level rise from salt-marsh sediments span the interval between
470 long term geological and recent instrumental records. Anthropogenic Pb emissions

preserved in salt-marsh sediment can be used as chronologic markers. Changing downcore Pb concentrations from a salt marsh in New Jersey, USA reflected prominent features in historic U.S. production and consumption at AD 1875, 1925, 1935 and 1974. Stable Pb isotopes transported by prevailing winds correlated with production in the Upper Mississippi Valley where Pb ores have an unusual and distinctively high ^{206}Pb:^{207}Pb ratio (AD 1827, 1857 and 1880). Changes in leaded gasoline are recognized at AD 1965 and 1980. These markers meet the need for geochronological horizons in the radiocarbon plateau of the last 400 years and also extend and independently corroborate accumulation histories derived from ^{210}Pb. Use of Pb concentrations and stable isotopes to date salt-marsh sediment helps extend high resolution sea-level reconstructions beyond the instrumental period of tide-gauge measurements and more precisely identify when modern rates of rise began.

Acknowledgements

Funding for this study was provided by NICRR grant DE-FC02-06ER64298, National Science Foundation award EAR-0951686 and NOAA grant NA11OAR4310101 (to B. Horton) and New Jersey Department of Environmental Protection Grant SR-0111 (to D. Velinsky and C. Sommerfield). C.H. Vane and S. Chenery publish with permission of the Executive Director of British Geological Survey. This research was supported by Earthwatch Institute Student Challenge Award Programs. Kemp thanks a post-doctoral fellowship at the Yale University Climate and Energy Institute. This paper is a contribution to IGCP project 588 "Preparing for coastal change" and PALSEA.

Comment [ak3]: Ben wanted to add a specific acknowledgement to Velinsky, what would be appropriate?

Figure Legends

Figure 1: Location of the Barnegat Bay study site in New Jersey, USA. Core BB1 has the geographic coordinates 40° 01.793' N, 74°04.797'W

Figure 2: Downcore measurements of stable Pb concentrations in Core BB1. (A) Gravimetric dry-bulk density. (B) Organic matter mass content estimated by loss on ignition (LOI). (C) Concentration of Pb (closed circles, black line) and Sb (open circles, grey line). (D) Measured ratio of ^{206}Pb to ^{207}Pb.

Figure 3: Downcore activity profiles of ^{210}Pb and ^{137}Cs. (A) Profile of excess ^{210}Pb with a fitted exponential curve and the accretion rate (*S*) computed following Eq. 1 in the text. (B) Profile of ^{137}Cs showing an activity peak presumed to be concordant with AD 1963-1964, and the accretion rate based in the age-depth relationship. Analytical uncertainity is smaller than symbol. (C) Age depth models developed for core BB1 using the ^{210}Pb CIC and CRS models. See text for description.

Figure 4: Historical records of Pb production and consumption. (A) U.S. Pb primary production and consumption. Data from the USGS Lead Statistical Compendium (AD 1830 to AD 1990) and the USGS Minerals Yearbook (AD 1991 to AD 2008). Vertical grey bands labeled A-D mark historic features used to assign ages to Pb concentrations in BB1. (B) Pb production from Upper Mississippi Valley ores (solid line from (Heyl et al., 1959), also shown as a percentage of the U.S. total (grey diamonds, right axis). Vertical

517 grey bands labeled E-G mark historic features used to assign ages to ^{206}Pb:^{207}Pb
518 variations in BB1 (C) Annual production of leaded gasoline in the U.S., redrawn from
519 (Nriagu, 1990).
520
521 **Figure 5:** Records of ^{206}Pb:^{207}Pb changes through time. (A, B) Historic fluctuations in
522 ^{206}Pb:^{207}Pb preserved in river basin (Pettaquamscutt, RI) and estuarine (Chesapeake Bay)
523 sediment cores and in annually-banded corals (Bermuda). Chronological control in each
524 case was from an independent dating method such as varve or band counting, ^{210}Pb or
525 pollen changes of known age. Changes in ^{206}Pb:^{207}Pb were not used as a dating
526 technique. (C) Historic record of ^{206}Pb:^{207}Pb in US leaded gasoline and atmospheric
527 measurements. The Anthropogenic Pb ArchaeoStratigraphy (ALAS) model (dashed line)
528 is reproduced from (Hurst, 2000). Data points are atmospheric measurements of
529 ^{206}Pb:^{207}Pb from locations in the USA (and in particular the northeast) reported by (1)
530 (Rosman et al., 1993) (2) (Shirahata et al., 1980) (3) (Sturges and Barrie, 1987) (4)
531 (Bollhöfer and Rosman, 2001). Vertical grey bands show inferred ages (H and I) for BB1
532 at AD 1965 and 1980.
533
534 **Figure 6:** Age-depth estimates for core BB-1. (A) Downcore changes in Pb
535 concentration (open circles) and ^{206}Pb:^{207}Pb ratios (filled squares) were used to assign
536 dates to specific depths on the basis of documented changes in national Pb production
537 and consumption and the contribution of Upper Mississippi Valley Pb with its unusual
538 isotopic signature. Isotopic changes at 34 cm could reflect maximum absolute production
539 in the Upper Mississippi Valley (AD 1846) or maximum proportional contribution (AD

1857), both are shown for comparison. Dashed grey line shows age-depth relationship from a constant initial concentration (CIC) model of ^{210}Pb accumulation that is supported by peak ^{137}Cs activity (grey square). It is restricted to the upper 27 cm of the core because at lower depths excess ^{210}Pb did not exceed analytical error. Vertical error bars represent sample thickness and uncertainty in selecting a single sample to assign an age to. Horizontal error bars represent uncertainty in assigning features in the historic record of Pb production an age, in most cases ± 5 years was used. (B) Age-depth model produced by "Clam" (Blaauw, 2010) using the nine horizons assigned ages based on changes in Pb concentration and ^{206}Pb:^{207}Pb ratio and the known age of the surface. A date of AD 1857 was used at 34 cm. The model was developed a locally-weighted spline function. Grey error band is the 95% confidence interval for estimated ages (solid line). CIC accumulation model developed from ^{210}Pb and ^{137}Cs is shown as a dashed grey line.

Table 1

	Year	Type	Description	Depth in BB1 (cm)	Age Error (yrs)
A	1875	Pb concentration	Start of national Pb production	33 ± 3	5
B	1925	Pb concentration	Peak in national Pb production	21 ± 1	5
C	1935	Pb concentration	Minimum in national Pb production and consumption	17 ± 1	6
D	1974	Pb concentration	Peak in national Pb production	9 ± 1	5
E	1827	^{206}Pb:^{207}Pb	Start of UMV Pb production	41 ± 1	5
F	1857.5	^{206}Pb:^{207}Pb	Peak contribution by UMV	34 ± 2	5
G	1880	^{206}Pb:^{207}Pb	Decline of UMV Pb production	25 ± 3	20
H	1965	^{206}Pb:^{207}Pb	Gasoline minimum	11 ± 1	5
I	1980	^{206}Pb:^{207}Pb	Gasoline peak	7 ± 1	5

Ages assigned to samples in core BB1 using measured lead concentrations and ^{206}Pb:^{207}Pb ratios in comparison with historical U.S. and Upper Mississippi Valley (UMV) lead production and consumption. Age error is an estimate of the uncertainty of identifying a specific date in historical records and is a minimum of 5 years to include a lag between Pb production and deposition. Depth has an uncertainty for sample thickness (±1 cm) and in some instances is larger because age horizons could be associated with a range of adjacent samples.

562 **References**

563
564 *Amarasiriwardena, D., Wu, F., 2011. Antimony: Emerging toxic contaminant in the*
565 *environment. Microchemical Journal 97, 1-3.*
566 *Appleby, P.G., 2001. Chronostratigraphic Techniques in Recent Sediments, In: Last,*
567 *W.M., Smol, J.P. (Eds.), Tracking Environmental Change Using Lake Sediments. Volume*
568 *1: Basin Analysis, Coring, and Chronological Techniques. Kluwer Academic Publishers,*
569 *Dordrecht, The Netherlands.*
570 *Appleby, P.G., Oldfield, F., 1992. Application of Lead-210 to Sedimentation Studies, In:*
571 *Ivanovich, M., Harmon, R.S. (Eds.), Uranium Series Disequilibrium: Applications to*
572 *Environmental Problems. Clarendon Press, pp. 731-778.*
573 *Ault, W.U., Senechal, R.G., Erlebach, W.E., 1970. Isotopic composition as a natural*
574 *tracer of lead in the environment. Environmental Science & Technology 4, 305-313.*
575 *Baker, J., Peate, D., Waight, T., Meyzen, C., 2004. Pb isotopic analysis of standards and*
576 *samples using a 207Pb-204Pb double spike and thallium to correct for mass bias with a*
577 *double-focusing MC-ICP-MS. Chemical Geology 211, 275-303.*
578 *Bennett, R.H., Lambert, D.N., 1971. Rapid and reliable technique for determining unit*
579 *weight and porosity of deep-sea sediments. Marine Geology 11, 201-207.*
580 *Blaauw, M., 2010. Methods and code for `classical' age-modelling of radiocarbon*
581 *sequences. Quaternary Geochronology 5, 512-518.*
582 *Bollhöfer, A., Rosman, K.J.R., 2000. Isotopic source signatures for atmospheric lead: the*
583 *Southern Hemisphere. Geochimica et Cosmochimica Acta 64, 3251-3262.*
584 *Bollhöfer, A., Rosman, K.J.R., 2001. Isotopic source signatures for atmospheric lead: the*
585 *Northern Hemisphere. Geochimica et Cosmochimica Acta 65, 1727-1740.*
586 *Cabanes, C., Cazenave, A., Le Provost, C., 2001. Sea Level Rise During Past 40 Years*
587 *Determined from Satellite and in Situ Observations. Science 294, 840-842.*
588 *Chapman, V.J., 1960. Salt Marshes and Salt Deserts of the World. Interscience*
589 *Publishers, New York.*
590 *Chillrud, S.N., Bopp, R.F., Ross, J.M., Chaky, D.A., Hemming, S., Shuster, E.L., Simpson,*
591 *H.J., Estabrooks, F., 2004. Radiogenic Lead Isotopes and Time Stratigraphy in the*
592 *Hudson River, New York. Water, Air, & Soil Pollution: Focus 4, 469-482.*
593 *Chillrud, S.N., Hemming, S., Shuster, E.L., Simpson, H.J., Bopp, R.F., Ross, J.M.,*
594 *Pederson, D.C., Chaky, D.A., Tolley, L.-R., Estabrooks, F., 2003. Stable lead isotopes,*
595 *contaminant metals and radionuclides in upper Hudson River sediment cores:*
596 *implications for improved time stratigraphy and transport processes. Chemical Geology*
597 *199, 53-70.*
598 *Chow, T.J., Earl, J.L., 1972. Lead Isotopes in North American Coals. Science 176, 510-*
599 *511.*
600 *Church, J., White, N., 2011. Sea-Level Rise from the Late 19th to the Early 21st Century.*
601 *Surveys in Geophysics, 1.*
602 *Church, J.A., White, N.J., 2006. A 20th century acceleration in global sea-level rise.*
603 *Geophysical Research Letters 33, L01602.*
604 *Cochran, J.K., Hirschberg, D.J., Wang, J., Dere, C., 1998. Atmospheric Deposition of*
605 *Metals to Coastal Waters (Long Island Sound, New York U.S.A.): Evidence from*
606 *Saltmarsh Deposits. Estuarine, Coastal and Shelf Science 46, 503-522.*

607 *Cutshall, N.H., Larsen, I.L., Olsen, C.R., 1983. Direct analysis of Pb-210 in sediment*
608 *samples: self-absorption corrections. Nuclear Instruments and Methods 206, 309-312.*
609 *Doe, B.R., 1970. Lead Isotopes. Springer-Verlag, Berlin.*
610 *Doe, B.R., Delevaux, M.H., 1972. Source of Lead in southeast Missouri Galena ores.*
611 *Economic Geology 67, 409-425.*
612 *Donnelly, J.P., Cleary, P., Newby, P., Ettinger, R., 2004. Coupling instrumental and*
613 *geological records of sea-level change: evidence from southern New England of an*
614 *increase in the rate of sea-level rise in the late 19th century. Geophysical Research*
615 *Letters 31, L05203.*
616 *Douglas, B.C., 2001. Sea-level rise in the era of the recording tide gauge, In: Douglas,*
617 *B.C., Kearney, M.S., Leatherman, S.P. (Eds.), Sea-level rise: history and consequences.*
618 *Academic Press, San Diego, pp. 37-64.*
619 *Edgington, D.N., Robbins, J.A., 1976. Records of lead deposition in Lake Michigan*
620 *sediments since 1800. Environmental Science & Technology 10, 266-274.*
621 *Engelhart, S.E., Peltier, W.R., Horton, B.P., 2011. Holocene relative sea-level changes*
622 *and glacial isostatic adjustment of the U.S. Atlantic coast. Geology 39, 751-754.*
623 *Engelhart, S.E., Horton, B.P., Douglas, B.C., Peltier, W.R., Tornqvist, T.E., 2009. Spatial*
624 *variability of late Holocene and 20th century sea-level rise along the Atlantic coast of the*
625 *United States. Geology 37, 1115-1118.*
626 *Facchetti, S., 1989. Lead in petrol. The isotopic lead experiment. Accounts of Chemical*
627 *Research 22, 370-374.*
628 *Farmer, J.G., Eades, L.J., Atkins, H., Chamberlain, D.F., 2001. Historical Trends in the*
629 *Lead Isotopic Composition of Archival Sphagnum Mosses from Scotland (1838â^'2000).*
630 *Environmental Science & Technology 36, 152-157.*
631 *Fujiwara, F.n., Rebagliati, R.l.J.n., Marrero, J., GÃ³mez, D., Smichowski, P., 2011.*
632 *Antimony as a traffic-related element in size-fractionated road dust samples collected in*
633 *Buenos Aires. Microchemical Journal 97, 62-67.*
634 *Gale, S.J., 2009. Event chronostratigraphy: A high-resolution tool for dating the recent*
635 *past. Quaternary Geochronology 4, 391-399.*
636 *Gehrels, W.R., Hayward, B., Newnham, R.M., Southall, K.E., 2008. A 20th century*
637 *acceleration of sea-level rise in New Zealand. Geophysical Research Letters 35, L02717.*
638 *Gehrels, W.R., Kirby, J.R., Prokoph, A., Newnham, R.M., Achterberg, E.P., Evans, H.,*
639 *Black, S., Scott, D.B., 2005. Onset of recent rapid sea-level rise in the western Atlantic*
640 *Ocean. Quaternary Science Reviews 24, 2083-2100.*
641 *Gomez, D.R., Fernanda Gine, M., Claudia Sanchez Bellato, A., Smichowski, P., 2005.*
642 *Antimony: a traffic-related element in the atmosphere of Buenos Aires, Argentina.*
643 *Journal of Environmental Monitoring 7, 1162-1168.*
644 *Graney, J.R., Halliday, A.N., Keeler, G.J., Nriagu, J.O., Robbins, J.A., Norton, S.A.,*
645 *1995. Isotopic record of lead pollution in lake sediments from the northeastern United*
646 *States. Geochimica et Cosmochimica Acta 59, 1715-1728.*
647 *Hamelin, B., Ferrand, J.L., Alleman, L., Nicolas, E., Veron, A., 1997. Isotopic evidence of*
648 *pollutant lead transport from North America to the subtropical North Atlantic gyre.*
649 *Geochimica et Cosmochimica Acta 61, 4423-4428.*
650 *Heiri, O., Lotter, A.F., Lemcke, G., 2001. Loss on ignition as a method for estimating*
651 *organic and carbonate content in sediments: reproducibility and comparability of results.*
652 *Journal of Paleolimnology 25, 101-110.*

Heyl, A.V., Landis, G.P., Zartman, R.E., 1974. Isotopic Evidence for the Origin of Mississippi Valley-Type Mineral Deposits: A Review. Economic Geology 69, 992-1006.
Heyl, A.V., Agnew, A., Lyons, E., Behre, C., 1959. The geology of the Upper Mississippi Valley lead-zinc district, USGS Professional Paper 309.
Heyl, A.V., Delevaux, M.H., Zartman, R.E., Brock, M.R., 1966. Isotopic study of galenas from the upper Mississippi Valley, the Illinois-Kentucky, and some Appalachian Valley mineral districts. Economic Geology 61, 933-961.
Hong, S., Candelone, J.-P., Patterson, C.C., Boutron, C.F., 1994. Greenland Ice Evidence of Hemispheric Lead Pollution Two Millennia Ago by Greek and Roman Civilizations. Science 265, 1841-1843.
Hua, Q., 2009. Radiocarbon: A chronological tool for the recent past. Quaternary Geochronology 4, 378.
Hua, Q., Barbetti, M., 2004. Review of tropospheric bomb (super 14) C data for carbon cycle modeling and age calibration purposes. Radiocarbon 46, 1273-1294.
Hurst, R.W., 2000. Applications of anthropogenic lead archaeostratigraphy (ALAS model) to hydrocarbon remediation. Environmental Forensics 1, 11-23.
Inn, K., Lin, Z., Wu, Z., McMahon, C., Filliben, J., Krey, P., Feiner, M., Liu, C.-K., Holloway, R., Harvey, J., Larsen, I., Beasley, T., Huh, C., Morton, S., McCurdy, D., Germain, P., Handl, J., Yamamoto, M., Warren, B., Bates, T., Holms, A., Harvey, B., Popplewell, D., Woods, M., Jerome, S., Odell, K., Young, P., Croudace, I., 2001. The NIST natural-matrix radionuclide standard reference material program for ocean studies. Journal of Radioanalytical and Nuclear Chemistry 248, 227-231.
Kamenov, G.D., Brenner, M., Tucker, J.L., 2009. Anthropogenic versus natural control on trace element and Sr-Nd-Pb isotope stratigraphy in peat sediments of southeast Florida (USA), ~1500 AD to present. Geochimica et Cosmochimica Acta 73, 3549-3567.
Kelly, A.E., Reuer, M.K., Goodkin, N.F., Boyle, E.A., 2009. Lead concentrations and isotopes in corals and water near Bermuda, 1780-2000. Earth and Planetary Science Letters 283, 93-100.
Kemp, A.C., Horton, B., Donnelly, J.P., Mann, M.E., Vermeer, M., Rahmstorf, S., 2011. Climate related sea-level variations over the past two millennia. Proceedings of the National Academy of Sciences 108, 11017-11022.
Kemp, A.C., Horton, B.P., Culver, S.J., Corbett, D.R., van de Plassche, O., Gehrels, W.R., Douglas, B.C., Parnell, A.C., 2009. Timing and magnitude of recent accelerated sea-level rise (North Carolina, United States). Geology 37, 1035-1038.
Kennish, M.J., 2001. Coastal Salt Marsh Systems in the U.S.: A Review of Anthropogenic Impacts. Journal of Coastal Research 17, 731-748.
Kennish, M.J., Bricker, S.B., Dennison, W.C., Gilbert, P.M., Livingston, R.J., Moore, K.A., Noble, R.T., Paerl, H.W., Ramstack, J.M., Seitzinger, S., Tomasko, D.A., Valiela, I., 2007. Barnegat Bay-Little Egg Harbor Estuary: case study of a highly eutrophic coastal bay system. Ecological applications 17, S3-S16.
Krishnaswamy, S., Lal, D., Martin, J.M., Meybeck, M., 1971. Geochronology of lake sediments. Earth and Planetary Science Letters 11, 407-414.
Leuliette, E.W., Miller, L., 2009. Closing the sea level rise budget with altimetry, Argo, and GRACE. Geophysical Research Letters 36, L04608.
Lima, A.L., Hubeny, J.B., Reddy, C.M., King, J.W., Hughen, K.A., Eglinton, T.I., 2005a. High-resolution historical records from Pettaquamscutt River basin sediments: 1. 210Pb

699 *and varve chronologies validate record of 137Cs released by the Chernobyl accident.*
700 *Geochimica et Cosmochimica Acta 69, 1803-1812.*
701 *Lima, A.L., Bergquist, B.A., Boyle, E.A., Reuer, M.K., Dudas, F.O., Reddy, C.M.,*
702 *Eglinton, T.I., 2005b. High-resolution historical records from Pettaquamscutt River*
703 *basin sediments: 2. Pb isotopes reveal a potential new stratigraphic marker. Geochimica*
704 *et Cosmochimica Acta 69, 1813-1824.*
705 *Marcantonio, F., Zimmerman, A., Xu, Y., Canuel, E., 2002. A Pb isotope record of mid-*
706 *Atlantic US atmospheric Pb emissions in Chesapeake Bay sediments. Marine Chemistry*
707 *77, 123-132.*
708 *Marshall, W.A., Gehrels, W.R., Garnett, M.H., Freeman, S.P.H.T., Maden, C., Xu, S.,*
709 *2007. The use of 'bomb spike' calibration and high-precision AMS C-14 analyses to date*
710 *salt-marsh sediments deposited during the past three centuries. Quaternary Research 68,*
711 *325-337.*
712 *McCaffery, R.J., Thomson, J., 1980. A record of accumulation of sediment and trace*
713 *metals in a Connecticut salt marsh, In: Saltzman, B. (Ed.), Estuarine physics and*
714 *chemistry: studies in Long Island Sond, 22 ed. Academic Press, New York, pp. 165-237.*
715 *McGee, E.J., Gallagher, D., Mitchell, P.I., Baillie, M., Brown, D., Keogh, S.M., 2004.*
716 *Recent chronologies for tree rings and terrestrial archives using 14C bomb fallout*
717 *history. Geochimica et Cosmochimica Acta 68, 2509-2516.*
718 *Nriagu, J.O., 1979. Global inventory of natural and anthropogenic emissions of trace*
719 *metals to the atmosphere. Nature 279, 409-411.*
720 *Nriagu, J.O., 1990. The rise and fall of leaded gasoline. The Science of The Total*
721 *Environment 92, 13-28.*
722 *Nriagu, J.O., 1998. PALEOENVIRONMENTAL RESEARCH:Enhanced: Tales Told in*
723 *Lead. Science 281, 1622-1623.*
724 *Orson, R.A., Warren, R.S., Niering, W.A., 1998. Interpreting sea-level rise and rates of*
725 *vertical marsh accretion in a southern New England tidal salt marsh. Estuarine, Coastal*
726 *and Shelf Science 47, 419-429.*
727 *Reimer, P.J., Reimer, R.W., 2007. Radiocarbon dating: calibration, In: Elias, R.W. (Ed.),*
728 *Encyclopedia of Quaternary Science. Elsevier, Amsterdam, pp. 2941-2950.*
729 *Robbins, J.A., 1978. Geochemical and geophysical applications of radioactive lead, In:*
730 *Nriagu, J.O. (Ed.), The biogeochemistry of lead in the environment. Elsevier, Amsterdam,*
731 *pp. 285-393.*
732 *Rosman, K.J.R., Chisholm, W., Boutron, C.F., Candelone, J.P., Gorlach, U., 1993.*
733 *Isotopic evidence for the source of lead in Greenland snows since the late 1960s. Nature*
734 *362, 333-335.*
735 *Rosman, K.J.R., Chisholm, W., Hong, S., Candelone, J.-P., Boutron, C.F., 1997. Lead*
736 *from Carthaginian and Roman Spanish Mines Isotopically Identified in Greenland Ice*
737 *Dated from 600 B.C. to 300 A.D.â€. Environmental Science & Technology 31, 3413-*
738 *3416.*
739 *Russell, R.D., Farquhar, R.M., 1960. Lead isotopes in Geology. Interscience, London.*
740 *Schaule, B.K., Patterson, C.C., 1981. Lead concentrations in the northeast Pacific:*
741 *evidence for global anthropogenic perturbations. Earth and Planetary Science Letters*
742 *54, 97-116.*
743 *Shen, G.T., Boyle, E.A., 1987. Lead in corals: reconstruction of historical industrial*
744 *fluxes to the surface ocean. Earth and Planetary Science Letters 82, 289-304.*

Shennan, I., Horton, B., 2002. Holocene land-and sea-level changes in Great Britain. Journal of Quaternary Science 17, 511-526.

Shirahata, H., Elias, R.W., Patterson, C.C., Koide, M., 1980. Chronological variations in concentrations and isotopic compositions of anthropogenic atmospheric lead in sediments of a remote subalpine pond. Geochimica et Cosmochimica Acta 44, 149-162.

Shotyk, W., Krachler, M., Chen, B., 2005. Antimony: global environmental contaminant. Journal of Environmental Monitoring 7, 1135-1136.

Shotyk, W., Goodsite, M.E., Roos-Barraclough, F., Frei, R., Heinemeier, J., Asmund, G., Lohse, C., Hansen, T.S., 2003. Anthropogenic contributions to atmospheric Hg, Pb and As accumulation recorded by peat cores from southern Greenland and Denmark dated using the ^{14}C "bomb pulse curve". Geochimica et Cosmochimica Acta 67, 3991-4011.

Shotyk, W., Weiss, D., Appleby, P.G., Cheburkin, A.K., Frei, R., Gloor, M., Kramers, J.D., Reese, S., Van Der Knaap, W.O., 1998. History of Atmospheric Lead Deposition Since 12,370 14C yr BP from a Peat Bog, Jura Mountains, Switzerland. Science 281, 1635-1640.

Sturges, W.T., Barrie, L.A., 1987. Lead 206/207 isotope ratios in the atmosphere of North America as tracers of US and Canadian emissions. Nature 329, 144-146.

Tornqvist, T.E., De Jong, A.F.M., Oosterbaan, W.A., Van der Borg, K., 1992. Accurate dating of organic deposits by AMS ^{14}C measurement of macrofossils. Radiocarbon 34, 566-577.

Tornqvist, T.E., Gonzalez, J.L., Newsom, L.A., van der Borg, K., de Jong, A.F.M., Kurnik, C.W., 2004. Deciphering Holocene sea-level history on the US Gulf Coast: a high-resolution record from the Mississippi Delta. Geological Society of America Bulletin 116, 1026-1039.

van de Plassche, O., van der Borg, K., de Jong, A.F.M., 1998. Sea level-climate correlation during the past 1400 yr. Geology 26, 319-322.

Vane, C.H., Chenery, S.R., Harrison, I., Kim, A.W., Moss-Hayes, V., Jones, D.G., 2011. Chemical signatures of the Anthropocene in the Clyde estuary, UK: sediment-hosted Pb, 207/206Pb, total petroleum hydrocarbon, polyaromatic hydrocarbon and polychlorinated biphenyl pollution records. Philosophical Transactions of the Royal Society A: Mathematical, Physical and Engineering Sciences 369, 1085-1111.

Velinsky, D.J., Sommerfield, C.K., Enache, M., Charles, D.F., 2011. Nutrient and ecological histories in Barnegat Bay, New Jersey. Patrick Center for Environmental Research, Academy of Natural Sciences of Philadelphia, Philadelphia.

Wallbrink, P.J., Walling, D.E., He, Q., 2002. Radionuclide measurement using HPGe gamma spectrometry, In: Zapata, F. (Ed.), Handbook for the Assessment of Soil Erosion and Sedimentation Using Environmental Radionuclides. Kluwer Academic, Dordrecht, pp. 67-96.

Woodworth, P.L., White, N.J., Jevrejeva, S., Holgate, S.J., Church, J.A., Gehrels, W.R., 2009. Evidence for the accelerations of sea level on multi-decade and century timescales. International Journal of Climatology 29, 777-789.

Wu, J., Boyle, E.A., 1997. Lead in the western North Atlantic Ocean: Completed response to leaded gasoline phaseout. Geochimica et Cosmochimica Acta 61, 3279-3283.

Wu, J., Rember, R., Jin, M., Boyle, E.A., Flegal, A.R., 2010. Isotopic evidence for the source of lead in the North Pacific abyssal water. Geochimica et Cosmochimica Acta 74, 4629-4638.

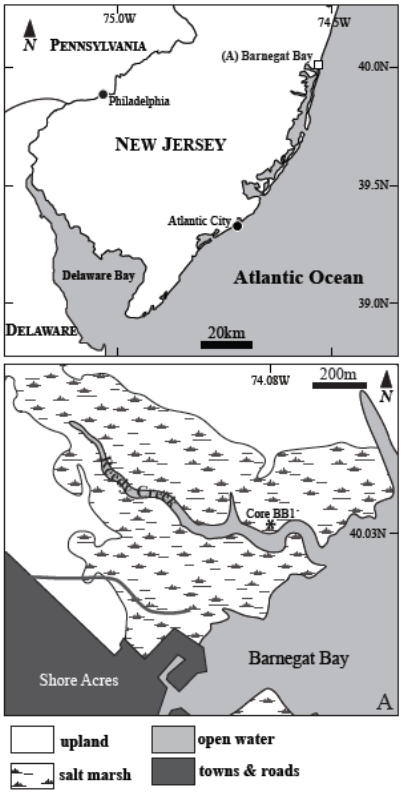

791
792
793
794
795
796
797
798
799
800
801
802
803
804
805
806
807
808
809

Figure 2

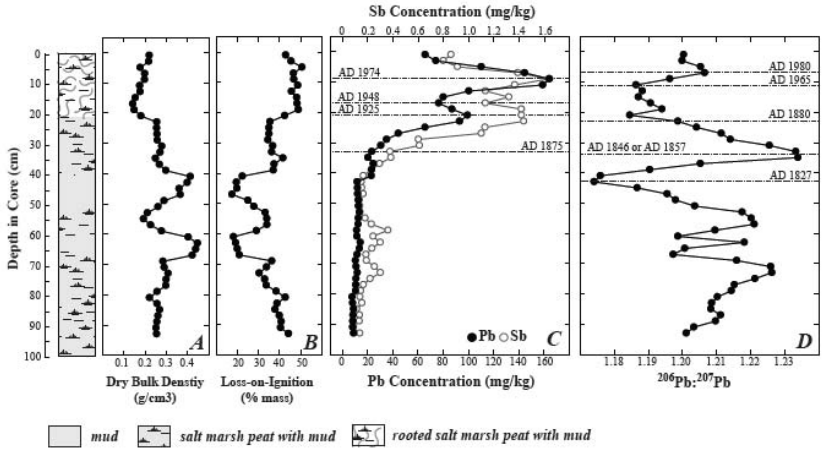
Sb Concentration (mg/kg)
Depth in Core (cm)
AD 1974
AD 1948
AD 1925
AD 1875
AD 1980
AD 1965
AD 1880
AD 1846 or AD 1857
AD 1827
Pb
Sb
A
B
C
D
Dry Bulk Denstiy (g/cm3)
Loss-on-Ignition (% mass)
Pb Concentration (mg/kg)
206Pb:207Pb
mud
salt marsh peat with mud
rooted salt marsh peat with mud

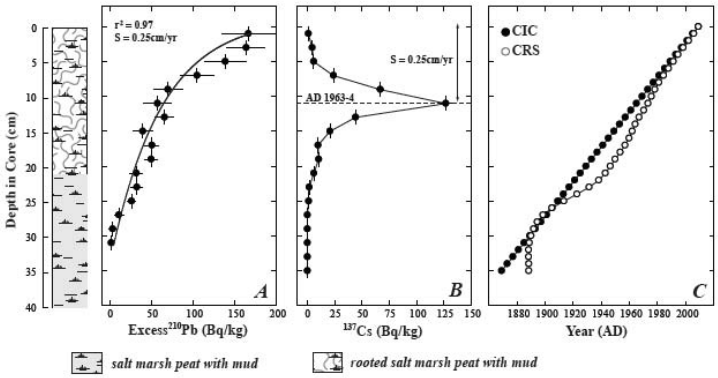

829
830
831
832
833
834
835
836
837
838

Figure 4

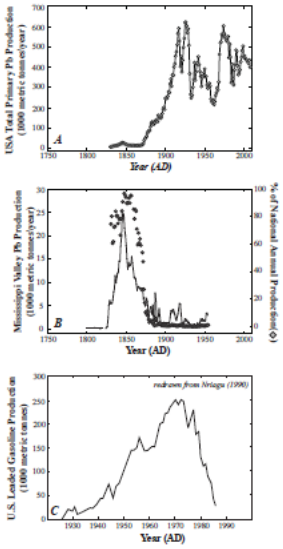
USA Total Primary Pb Production (1000 metric tonnes/year)
A
Year (AD)
Mississippi Valley Pb Production (1000 metric tonnes/year)
% of N.Atlantic Annual Pb Production
B
Year (AD)
redrawn from Nriagu (1990)
U.S. Leaded Gasoline Production (1000 metric tonnes)
C
Year (AD)

Figure 5

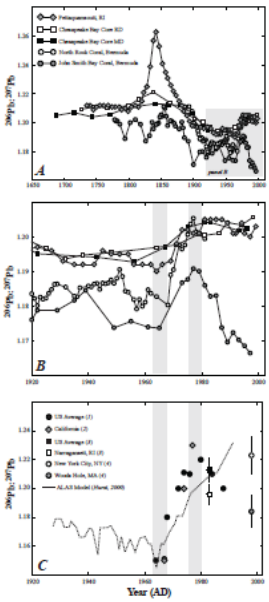

845
846
847
848
849

Figure 6

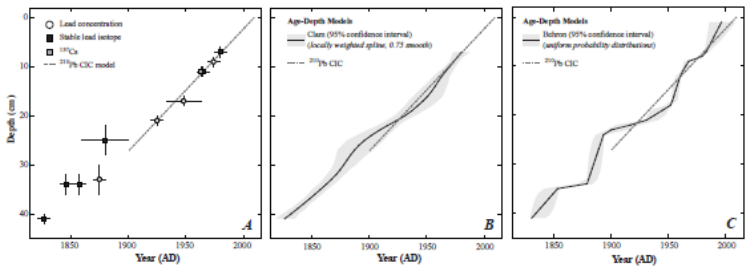

850